

Published in final edited form as:

Bioorg Med Chem Lett. 2014 February 15; 24(4): 1148–1153. doi:10.1016/j.bmcl.2013.12.122.

A novel class of ion displacement ligands as antagonists of the α IIb β 3 receptor that limit conformational reorganization of the receptor

Jian-kang Jiang¹, Joshua G. McCoy¹, Min Shen¹, Christopher A. LeClair¹, Wenwei Huang¹, Ana Negri², Jihong Li³, Robert Blue³, Amanda Weil Harrington³, Sarasija Naini³, George David III³, Won-Seok Choi³, Elisabetta Volpi³, Joseph Fernandez⁴, Mariana Babayeva⁵, Mark A. Nedelman⁶, Marta Filizola², Barry S. Coller³, and Craig J. Thomas^{*,1}

¹ NIH Chemical Genomics Center, Division of Preclinical Innovation, National Center for Advancing Translational Sciences, National Institutes of Health, Bethesda, MD

² Department of Structural and Chemical Biology, Icahn School of Medicine at Mount Sinai, New York, NY

³ Allen and Frances Adler Laboratory of Blood and Vascular Biology, Rockefeller University, New York, NY

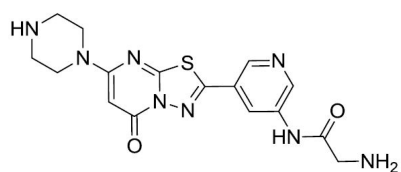
⁴ Proteomics Resource Center, Rockefeller University, New York, NY

⁵ Touro College of Pharmacy, New York, NY

⁶ Ekam Imaging, Boston, MA

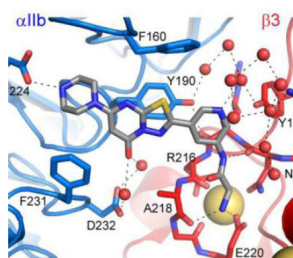
Abstract

A collection of α IIb β 3 integrin receptor antagonists possessing a unique MIDAS metal ion displacement mechanism of action is presented. Insight into these agents' structure-activity relationships, binding modality, and pharmacokinetic and pharmacodynamic profiles highlight the potential of these small molecule ion displacement ligands as attractive candidates for clinical development.



13

Platelet Aggregation (IC₅₀): 0.045 μ M



*Corresponding author: Craig J. Thomas NIH Chemical Genomics Center National Center for Advancing Translational Sciences National Institutes of Health Bethesda, MD 20892, USA craigt@mail.nih.gov Tel: + 1-301-217-4079 Fax: +1-301-217-5736.

Publisher's Disclaimer: This is a PDF file of an unedited manuscript that has been accepted for publication. As a service to our customers we are providing this early version of the manuscript. The manuscript will undergo copyediting, typesetting, and review of the resulting proof before it is published in its final citable form. Please note that during the production process errors may be discovered which could affect the content, and all legal disclaimers that apply to the journal pertain.

Supporting Information

Supplementary data associated with this article can be found, in the online version, at...

The α IIb β 3 integrin receptor is an important mediator of platelet aggregation and to date three α IIb β 3 antagonists have been approved for human use by the U.S. Food and Drug Administration, including the small molecules eptifibatide and tirofiban (Figure 1).¹⁻³ Integrin receptors are heterodimeric complexes that rely upon coordinated conformational changes to the α and β subunits to initiate ligand binding, and upon ligand binding to convey signals to within cells that ultimately alter a wide array of phenotypes ranging from cytoskeletal reorganization, to cellular differentiation, to specified immune responses.⁴ The use of α IIb β 3 antagonists to alter platelet aggregation results in clinical utility for these agents as antithrombotic therapies. The aforementioned small molecule α IIb β 3 antagonists are modeled after the Arg-Gly-Asp (RGD) motif found in some of the naturally occurring ligands.⁵ The binding of both eptifibatide and tirofiban are particularly reliant upon interactions with a conserved Asp (224) residue found in the α IIb subunit and span a defined binding pocket to also engage a Mg²⁺ ion found in the β 3 subunit's metal ion-dependent adhesion site (MIDAS) domain.^{5,6} Crystallographic analysis of these drugs (and other RGD mimetics) demonstrates that after these antagonists (and a related peptide from the ligand fibrinogen) bind, the β 3 unit undergoes a 'swing-out' motion resulting in a major change in conformation.⁵⁻⁸ This conformational change has been theorized to contribute to the thrombocytopenia caused by the RGD mimetic agents by exposing neopeptides for which some individuals have pre-formed antibodies.⁹ Attempts to develop oral RGD mimetic agents to inhibit α IIb β 3 failed because the agents produced thrombocytopenia and some were associated with a paradoxical increase in mortality.^{10,11} This latter effect has been theorized to be due to these agents' ability to "prime" the receptor to bind fibrinogen as the conformational change induced by the agents leaves the receptor in a high affinity ligand binding state.^{3,11-15} Thus, while α IIb β 3 represents a validated drug target, there remains a need to identify small molecule α IIb β 3 antagonists that do not alter the β 3 subunit conformation since these may have better safety profiles.

In an attempt to identify a novel small molecule capable of retaining the advantageous physiological effects associated with α IIb β 3 receptor antagonism without the negative consequences of receptor 'priming' we screened and identified a novel 5H-[1,3,4]thiadiazolo[3,2-a]pyrimidin-5-one based small molecule antagonist.¹⁶ This agent, named RUC-1 (**1**, Figure 1), was found to inhibit adhesion of platelets to fibrinogen and block ADP-induced platelet aggregation at modest potencies. It was also noted that **1** was selective for the α IIb β 3 receptor over related integrins α V β 3 and α 2 β 1 and for human α IIb β 3 over murine and rat α IIb β 3.^{16,17} The specificity for human α IIb β 3 resided in the α IIb subunit and thus its antithrombotic properties could be determined in a transgenic murine model in which mice express human α IIb in complex with murine β 3 (h α IIb/m β 3).^{16,17} Intriguingly, the β 3 domain of the receptor was shown to undergo little or no swing-out and the receptor did not undergo priming upon compound binding when compared with eptifibatide and tirofiban binding.¹⁶⁻¹⁸ An X-ray crystallographic analysis of this agent bound to the α IIb β 3 receptor confirmed molecular dynamic (MD) simulations suggesting that **1** bound exclusively to the α IIb domain of the receptor (PDB codes: 3NID, 3NIG, 3NIF).¹⁸ Pharmacokinetic studies conducted in dogs demonstrated rapid oral absorption (T_{max} \approx 0.5 hr), high oral bioavailability (\sim 92%), and rapid elimination (t_{1/2} \approx 2hr)(Table S1).

To optimize this agent a series of analogues were synthesized and examined for improved potency in the aforementioned platelet/fibrinogen adhesion and platelet aggregation assays. From these efforts, an analogue of **1** named RUC-2 (**2**, ML165, Figure 1) was identified that possessed increased affinity for the receptor and maintained the favorable lack of effect on receptor conformation as judged by several analyses, including electron microscopy of α IIb β 3 nanodiscs, Stokes radii measurements by gel filtration, exposure of ligand-induced binding site epitopes for monoclonal antibodies, and dynamic light scattering.¹⁹ Importantly,

2 also did not prime the receptor to fibrinogen binding nor in the majority of cases, induce recruitment to platelets of α IIb β 3-dependent antibodies from the serum of patients who developed thrombocytopenia when treated with eptifibatid or tirofiban.¹⁹ X-ray crystallographic studies revealed that **2** possessed a unique binding modality whereby the primary amine of the chemical structure of the ligand replaced the Mg²⁺ found within the MIDAS domain by binding to Glu220, one of the major Mg²⁺ coordinating residues (PDB code: 3T3M).¹⁹ This agent represents the first in a novel pharmacological class, which we term “ion displacement ligands” with remarkable selectivity and a lack of detrimental conformational events for the ligand-bound receptor. Here, we detail the structure-activity relationships (SAR) revealed during the optimization effort, highlight additional MD simulations that underscore the unique binding of this class of molecules and provide pharmacokinetic (PK) parameters for advanced analogues.

The optimization of **1** focused on structural alteration to the piperazine domain and the 2- and 6-positions of the core 5H-[1,3,4]thiadiazolo[3,2-a]pyrimidin-5-one heterocycle. Numerous analogues were synthesized and tested and a collection of representative SAR is presented in table 1. It rapidly became apparent that the secondary amine of the piperazine domain would not tolerate alteration as judged by conversions to piperidine (analogue **3**), morpholine (analogue **4**) and *N*-methyl-piperazine (analogue **5**). These results were consistent with the crystallographic analysis that demonstrated the key interaction of this moiety with α IIb Asp224.¹⁸ All additional attempts to alter the piperazine ring system led to a loss in activity, including steric additions to the 2- and 6-positions (for instance 2,6-dimethylpiperazine), bicyclic analogues (for instance 2,5-diazabicyclo[2.2.2]octane), alternate diamines (for instance *N*-phenylazetidid-3-amine), and selected spirocyclic compounds (for instance 2,7-diazaspiro[4.4]nonane)(data not shown). Changes to the 2-position of the 5H-[1,3,4]thiadiazolo[3,2-a]pyrimidin-5-one were limited to fluorine and selected alkyl groups (R2 in Table 1). A methyl group at this domain remained active (slight loss in activity) while any larger substitution resulted in an inactive analogue (data not shown). The fluorine substitution (analogue **6**) retained equivalent activity to that of **1**. Changes to the 6-position of the heterocycles included modified alkyl and aryl groups. Changing from the ethyl in **1** to a *tert*-butyl (analogue **7**) produced an agent with equivalent activity as did the phenyl analogue **8**. Multiple ring substitutions on the phenyl ring were explored including carboxylic acids (analogues **9** and **10**). In general, potencies for these agents were equivalent to that displayed by **1**. Incorporation of a 2-aminoacetamide at the meta position of the phenyl ring (analogue **2**), however, produced a striking increase in potency in both the adhesion assay (83% at 1 μ M) and the aggregation assay (0.096 μ M). The aforementioned crystallographic analysis identified the novel interaction between **2** and the MIDAS domain¹⁹ and we endeavored to fully explore the SAR of this new binding modality. Interestingly, a single methyl group on the alkyl chain [(*S*)-2-aminopropanamide] (analogue **12**) results in a significant loss in activity. This result conforms to the crystallographic analysis that demonstrates a limited amount of free space as the amide NH forms a key hydrogen bond with the backbone Asn215 carbonyl, resulting in proximal binding to Asn215 limiting the required space for the incorporated methyl group. Furthermore, additional bulk placed upon the primary amine (data not shown) eliminated activity. Again, crystallographic analysis of **2** highly suggests that the replacement of the Mg²⁺ ion by the primary amine allows for a nearly identical conformation for the amino acid side-chains that define the MIDAS domain and mitigates any alteration to this key pharmacophore. Modification of the phenyl ring (substitutions X2 and X3 in Table 1) maintained similar activity and selected analogues incorporating ring nitrogens [**13** and **14**] provided slight increases in potency and improved key physicochemical properties (see below). Based upon the modest potency enhancement demonstrated by **13** and on selected pharmacokinetic and pharmacodynamic studies with this agent, we further confirmed that **13**

neither primes the receptor for fibrinogen binding nor changes the $\beta 3$ conformation as judged by the binding of a conformation-specific monoclonal antibody; it also does not possess any activity versus the $\alpha V\beta 3$ receptor suggesting a high degree of selectivity for $\alpha IIb\beta 3$ akin to our studies with **2** (manuscript in preparation).¹⁹

We previously reported the synthesis of **2** from an 5-(3-nitrophenyl)-1,3,4-thiadiazol-2-amine (see reference 19). Analogues reported here-in, including **13** were synthesized utilizing the same protocol from commercially available materials [for instance, 5-nitronicotinic acid for the production of **13** (Scheme S1)]. To facilitate the multiple follow-up studies undertaken with **13** we optimized this route utilizing 5-bromonicotinic acid (Scheme 1). Conversion to the acid chloride followed by addition of hydrazinecarbothioamide yielded the required acyl-hydrazinecarbothioamide (**17**) in greater than 50% yield over two steps. Addition of **17** to PPA at 100 °C cleanly formed the 1,3,4-thiadiazol-2-amine **18** which was converted to the 7-chloro-5H-[1,3,4]thiadiazolo[3,2-a]pyrimidin-5-one **19** by condensing with methyl-3-chloro-3-oxopropanoate followed by chlorination via $POCl_3$ treatment. Nucleophilic displacement of the 3-chloro moiety with 1-Boc-piperazine was followed by a Buchwald-Hartwig amination using Boc-protected 2-aminoacetamide which proceeded with an 80% yield. Treatment with TFA afforded deprotection of both Boc protecting groups.

To better understand the subtle improvement in potency found through incorporation of the ring nitrogens into the core of **2** we carried out molecular dynamic simulations of the integrin $\alpha IIb\beta 3$ headpiece bound to **2**, **13**, or analogue **14**. Starting from the crystallographic pose of **2**, each agent's initial geometry was optimized *ab initio* using a restricted Hartree-Fock (RHF) calculation with a 6-31G (d) basis set, as implemented in the Gaussian 09 program,²⁰ and the resulting geometries used to calculate electrostatic potential-derived (ESP) point charges employing the RESP methodology, as implemented in the AMBER suite of programs,²¹ and reported previously.¹⁹ Ligands were then docked in an equivalent geometric orientation within the binding pocket to that seen in the crystal structure of the **2**- $\alpha IIb\beta 3$ headpiece. All three resulting $\alpha IIb\beta 3$ headpiece-drug systems, including the SyMBS and ADMIDAS Ca^{2+} metal ions and the crystallographic water molecules found in all metal binding sites, were immersed in truncated octahedral boxes of ~22,000 TIP3P water molecules and neutralized by the addition of 7 Na^+ counter-ions at random locations. Each system was simulated for 20 ns by all-atom, standard MD simulations, using the general AMBER force field (GAFF) for the ligands and the ff12SB force field for the protein, within the AMBER12.0 suite of programs.²¹

Detailed analysis of representative snapshots from the 20 ns simulation trajectories of **2**- $\alpha IIb\beta 3$ (Figure 2, panel A), **14**- $\alpha IIb\beta 3$ (Figure 2, panel B), and **13**- $\alpha IIb\beta 3$ (Figure 2, panel C) shows that both **14** and **13** maintain a similar geometry to the pose adopted by **2** during dynamics. Stable interactions monitored during simulations included the piperazine-Asp224 hydrogen bond, the primary amine interactions with Glu220 and the backbone carbonyl oxygen of Asp218, and a hydrogen bond between the phenylacetamide and the backbone carbonyl oxygen of $\beta 3$ Asn215. We additionally noted a stable π - π stacking interaction between each of the compounds' fused ring and the αIIb Tyr190 aromatic ring and a water-mediated hydrogen bond between the carbonyl group in each of the compounds' fused ring and the side chain carboxyl group of αIIb Asp232. The average distances between the aforementioned atoms and protein residues monitored during simulation are reported in Supplemental Table 2. There are no direct interactions between residues of the $\alpha IIb\beta 3$ headpiece and **13** and **14** that are not also present in **2**, making understanding of the slight potency enhancement for these agents not obvious. There are additional water-mediated interactions between the inserted ring nitrogen in **13** and Tyr166 that may differentiate the binding of this congener from that of **2** (Figure 2). Similarly, the inserted nitrogen in **14**

appears to support additional water-mediated interactions with Tyr166 and Arg214 (Figure 2B). These additional water-mediated interactions with the $\beta 3$ subunit may account for the slightly higher affinity of **13** and **14** relative to **2**.

The novel binding modality demonstrated by these agents make them ideal probe molecules for further study of ion-displacement antagonists as a novel means of pharmacological intervention. We were also interested in examining **2** and its structural congeners for potential translation into clinical reagents. Given the limitations associated with the current approved drugs there is a need to develop novel α IIB β 3 antagonists that possess the appropriate combination of attributes to establish them as new drugs. As such, we examined key analogues for selected physicochemical and preclinical ADME properties. From the outset, we prioritized **2**, **13** and **14** for advanced study. Prior to ADME analysis we noted that **14** possessed poor chemical stability as a solution (both DMSO-based and aqueous) and consequently this analogue was deprioritized. Initial assessments included an analysis of the aqueous solubility and biological stability of **2** and **13** (Table 2). Both analogues were highly stable in mouse plasma and each agent possessed a positive solubility profile across a range of pH values. Neither eptifibatide nor tirofiban possess oral bioavailability, which may be attributed to their having formal positively and negatively charged elements in their chemical structure. Likewise, **2** and **13** are charged drugs at physiological pH (pKa values for **2** were experimentally determined at 6.41 and 8.08) and thus, as expected, PAMPA and Caco2 permeability analyses indicated that it was unlikely that either agent possesses high oral bioavailability (data not shown). However, the intended clinical application for this agent is in the early, pre-hospital treatment of patients with myocardial infarction in hopes of ameliorating the mortality and morbidity by decreasing the resulting tissue death and long-term cardiac dysfunction. Several studies have explored the use of α IIB β 3 antagonists in a pre-hospital setting and present evidence that such therapeutic intervention translates into both acute and long-term benefit.²²⁻²⁴ To apply novel α IIB β 3 antagonists in such a setting requires a facile administration route and method of delivery. The anticipated use of autoinjector technology to provide a bolus dose of drug via IM injection would provide a means to deliver an anticipated dose (~ 1 mg/kg) of drug. Autoinjectors are limited in their volume of delivery and therefore require the API to possess significant solubility in the delivery vehicle (a primarily aqueous formulation). Both **2** and **13** are soluble small organic molecules as judged by both kinetic and thermodynamic solubility assessments, but **13** is much more soluble as judged by chemiluminescent nitrogen detection (CLND)(Table 2) and, in fact, many of the measured values exceeded the detection limit of these methods. An LC method was also performed and correlated well with the data shown in Table 2. Additional studies have demonstrated that **13** can be solubilized long-term up-to and exceeding levels of 60 mg/mL, which far exceeds the level that can be achieved for **2**. As a result, for the ideal delivery mechanism, **13** represents a strong candidate agent.

Effort was also put forth to examine several predictive in vitro toxicology markers. Both **2** and **13** were further profiled for hERG inhibition with neither agent presenting activity versus this common target at all concentrations tested. As these agents represent cationic, amphiphilic drugs we also examined the capacity of **13** to produce a drug-induced phospholipidosis event.²⁵ No appreciable induction of phospholipidosis was noted nor did **13** alter nuclear size or induce stenosis (data not shown). The fraction unbound (f_u) for **13** in both whole blood and plasma protein was high (>85% and >30%, respectively; data not shown).

An analysis of the microsomal stability for **2** and **13** suggested that **2** was highly resistant to metabolism in three species (mouse, rat and human microsomes) while **13** possessed a more modest stability profile. Hepatocyte stability (mouse) was also assessed for **13** and found to be negligible (>95% remaining after 120 minutes). The exposure (PK) profile for each agent

(both IV and IP administration route) suggested that each agent has a rapid onset and a limited time of exposure following a dose of 0.03 mgs. These data are generally contradictory to the microsomal stability results, suggesting an alternate route of metabolism/clearance. The limited exposure times are beneficial for use in the proposed pre-hospital infarction indication where a drug-induced antiplatelet effect is desired for a limited time interval, thus allowing first responders to administer drug without preventing the physicians in the receiving hospital from instituting whichever drugs and interventions they think best.

In summary, we report the discovery and optimization of a novel class of α IIb β 3 antagonists that demonstrate a novel ion displacement mechanism of action. This binding modality allows our lead agents **2** and **13** to inhibit receptor function without significant β 3 conformational reorganization, thus avoiding receptor priming and perhaps decreasing the likelihood of developing thrombocytopenia. Our results suggest that advanced analogues **13** and **14** bind to the protein in a similar fashion as **2** with additional water-mediated interactions that potentially account for modest affinity gains. Neither **2** nor **13** possess any predictive toxicology liabilities and **13** possesses both the required aqueous solubility and chemical properties for the specified clinical applications. Pharmacodynamic analysis of both **2** and **13** in an engineered mouse model and **13** in a non-human primate model (manuscript in preparation), support the advancement of this class of α IIb β 3 antagonists into advanced preclinical studies.

Supplementary Material

Refer to Web version on PubMed Central for supplementary material.

Acknowledgments

The authors thank Jim Bougie, Thomas Daniel and William Leister for compound purification, as well as Paul Shinn, Danielle VanLeer for assistance with compound management. This research was supported by the Molecular Libraries Initiative of the National Institutes of Health Roadmap for Medical Research grant U54HG005033 and the Intramural Research Program of the National Human Genome Research Institute at the National Institutes of Health. This work was further supported, in part, by grants HL19278, HL13629, and HL48675, and from the National Heart, Lung, and Blood Institute, and CTSA grant ULRR024143 from the National Center for Research Resources, NIH. Computations were run, in part, on resources available through the Scientific Computing Facility at Icahn School of Medicine at Mount Sinai and in part on TeraGrid advanced computing resources provided by Texas Advanced Computing Center through TG-MCB080077.

References

1. Bledzka K, Smyth SS, Plow EF. Integrin α IIb β 3: From discovery to efficacious therapeutic target. *Circ. Res.* 2013; 112:1189–1200. [PubMed: 23580774]
2. Lang SH, Manning N, Armstrong N, Misso K, Allen A, Di Nisio M, Kleijnen J. Treatment with tirofiban for acute coronary syndrome (ACS): a systematic review and network analysis. *Curr. Med. Res. Opin.* 2012; 28:351–370. [PubMed: 22292469]
3. Collier BS, Shatil SJ. The GPIIb/IIIa (integrin α IIb β 3) odyssey: A technology-driven saga of a receptor with twists, turns and even a bend. *Blood.* 2008; 112:3011–3025. [PubMed: 18840725]
4. Hynes RO. Integrins: bi-directional, allosteric, signaling machines. *Cell.* 2002; 110:673–687. [PubMed: 12297042]
5. Xiao T, Takagi J, Collier BS, Wang JH, Springer TA. Structural basis for allostery in integrins and binding to fibronectin-mimetic therapeutics. *Nature.* 2004; 432:59–67. [PubMed: 15378069]
6. Luo BH, Carman CV, Springer TA. Structural basis of integrin regulation and signaling. *Annu. Rev. Immunol.* 2007; 25:619–647. [PubMed: 17201681]
7. Springer TA, Zhu J, Xiao T. Structural basis for distinctive recognition of fibrinogen by the platelet integrin α IIb β 3. *J. Cell Biol.* 2008; 182:791–800. [PubMed: 18710925]

8. Takagi J, Petre BM, Walz T, Springer TA. Global conformational rearrangements in integrin extracellular domains in outside-in and inside out signaling. *Cell*. 2002; 110:599–611. [PubMed: 12230977]
9. Bougie DW, Wilker PR, Uuitchick ED, Curtins BR, Malik M, Levine S, Lind RN, Pereira J, Aster RH. Acute thrombocytopenia after treatment with tirofiban or eptifibatid is associated with antibodies specific for ligand-occupied GPIIb/IIIa. *Blood*. 2002; 100:2017–2076.
10. Chew DP, Bhatt DL, Topol EJ. Oral glycoprotein IIb/IIIa inhibitors: why don't they work? *Am. J. Cardiovasc. Drugs*. 2001; 1:421–428. [PubMed: 14728001]
11. Cox D. Oral GPIIb/IIIa antagonists: what went wrong? *Curr. Pharm. Des.* 2004; 10:1587–1596. [PubMed: 15134557]
12. Du XP, Plow EF, Frelinger AL 3rd, O'Toole TE, Loftus JC, Ginsberg MH. Ligands 'activate' integrin alpha IIb beta 3 (platelet GPIIb-IIIa). *Cell*. 1991; 65:409–416. [PubMed: 2018974]
13. Hantgan RR, Stahle MC. Integrin priming dynamics: mechanisms of integrin antagonist-promoted alphaIIb beta3: PAC-1 molecular recognition. *Biochemistry*. 2009; 48:8355–8365. [PubMed: 19640007]
14. Jones ML, Harper MT, Aitken EW, Williams CM, Poole AW. RGD-ligand mimetic antagonists of integrin alphaIIb beta3 paradoxically enhance GPVI-induced human platelet activation. *J. Thromb. Haemost.* 2010; 8:567–576. [PubMed: 20002543]
15. Bassler N, Loeffler C, Mangin P, Yuan Y, Schwarz M, Hagemeyer CE, Eisenhardt SU, Ahrens I, Bode C, Jackson SP, Peter K. A mechanistic model for the paradoxical platelet activation by ligand-mimetic alphaIIb beta3 (GPIIb/IIIa) antagonists. *Arterioscler. Thromb. Vasc. Biol.* 2007; 27:e9–e15. [PubMed: 17170374]
16. Blue R, Murcia M, Karan C, Jirousková M, Collier BS. Application of high-throughput screening to identify a novel alphaIIb-specific small-molecule inhibitor of alphaIIb beta3-mediated platelet interaction with fibrinogen. *Blood*. 2008; 111:1248–1256. [PubMed: 17978171]
17. Blue R, Kowalska MA, Hirsch J, Murcia M, Janczak CA, Harington M, Jirousková M, Li J, Fuentes R, Thornton MA, Filizola M, Poncz M, Karan C, Collier BS. Structural and therapeutic insights from the species specificity and in vivo antithrombotic activity of a novel alphaIIb-specific alphaIIb beta3 antagonist. *Blood*. 2009; 114:195–201. [PubMed: 19414864]
18. Zhu J, Zhu J, Negri A, Provasi D, Filizola M, Collier BS, Springer TA. Closed headpiece of integrin alphaIIb beta3 and its complex with an alphaIIb beta3-specific antagonist that does not induce opening. *Blood*. 2010; 116:5050–5059. [PubMed: 20679525]
19. Zhu J, Choi W-S, McCoy JG, Negri A, Zhu J, Naini S, Li J, Shen M, Huang W, Bougie D, Rasmussen M, Aster R, Thomas CJ, Filizola M, Springer TA, Collier BS. Structure-guided design of a high-affinity platelet integrin alphaIIb beta3 receptor antagonist that disrupts Mg²⁺ binding to the MIDAS. *Science Trans. Med.* 2012; 4:125ra32.
20. Frisch, MJ.; Trucks, GW.; Schlegel, HB.; Scuseria, GE.; Robb, MA.; Cheeseman, JR.; Montgomery, JAJ.; Vreven, T.; Kudin, KN.; Burant, JC.; Millam, JM.; Iyengar, SS.; Tomasi, J.; Barone, V.; Mennucci, B.; Cossi, M.; Scalmani, G.; Rega, N.; Petersson, GA.; Nakatsuji, H.; Hada, M.; Ehara, M.; Toyota, K.; Fukuda, R.; Hasegawa, J.; Ishida, M.; Nakajima, T.; Honda, Y.; Kitao, O.; Nakai, H.; Klene, M.; Li, X.; Knox, JE.; Hratchian, HP.; Cross, JB.; Bakken, V.; Adamo, C.; Jaramillo, J.; Gomperts, R.; Stratmann, RE.; Yazyev, O.; Austin, AJ.; Cammi, R.; Pomelli, C.; Ochterski, JW.; Ayala, PY.; Morokuma, K.; Voth, GA.; Salvador, P.; Dannenberg, JJ.; Zakrzewski, VG.; Dapprich, S.; Daniels, AD.; Strain, MC.; Farkas, O.; Malick, DK.; Rabuck, AD.; Raghavachari, K.; Foresman, JB.; Ortiz, JV.; Cui, Q.; Baboul, AG.; Clifford, S.; Cioslowski, J.; Stefanov, BB.; Liu, G.; Liashenko, A.; Piskorz, P.; Komaromi, I.; Martin, RL.; Fox, DJ.; Keith, T.; Al-Laham, MA.; Peng, CY.; Nanayakkara, A.; Challacombe, M.; Gill, PMW.; Johnson, B.; Chen, W.; Wong, MW.; Gonzalez, C.; Pople, JA. Gaussian 03, Revision C.02. Gaussian, Inc.; Wallingford CT: 2004.
21. <http://ambermd.org/>
22. DE Luca G, Bellandi F, Huber K, Noc M, Petronio AS, Arntz HR, Maioli M, Gabriel HM, Zorman S, DE Carlo M, Rakowski T, Gyongyosi M, Dudek D. Early glycoprotein IIb-IIIa inhibitors in primary angioplasty-abciximab long term results (EGYPT-ALT) cooperation: individual patient's data meta-analysis. *J. Thromb. Haemost.* 2011; 9:2361–2370. [PubMed: 21929513]

23. Xu Q, Yin J, Si LY. Efficacy and safety of early versus late glycoprotein IIb/IIIa inhibitors for PCI. *Int. J. Cardiol.* 2013; 162:210–219. [PubMed: 22769575]
24. Hassan AK, Liem SS, van der Kley F, Bergheanu SC, Wolterbeek R, Bosch J, Bootsma M, Zeppenfeld K, van der Laarse A, Atsma DE, Jukema JW, Schalij MJ. In-ambulance abciximab administration in STEMI Patients prior to primary PCI is associated with smaller infarct size, improved LV function and lower incidence of heart failure: results from the Leiden MISSION! Acute myocardial infarction treatment optimization program. *Catheter Cardiovasc. Interv.* 2009; 74:335–343. [PubMed: 19642182]
25. Anderson N, Borlak J. Drug-induced phospholipidosis. *FEBS Lett.* 2006; 580:5533–5540. [PubMed: 16979167]

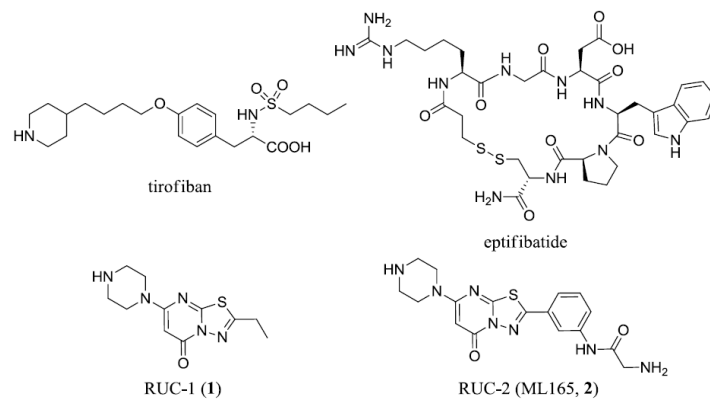


Figure 1.
Chemical structures of tirofiban, eptifibatid, RUC1 (1) and RUC2 (ML165, 2).

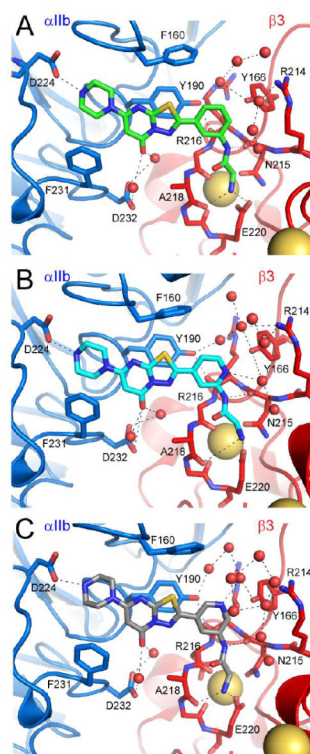
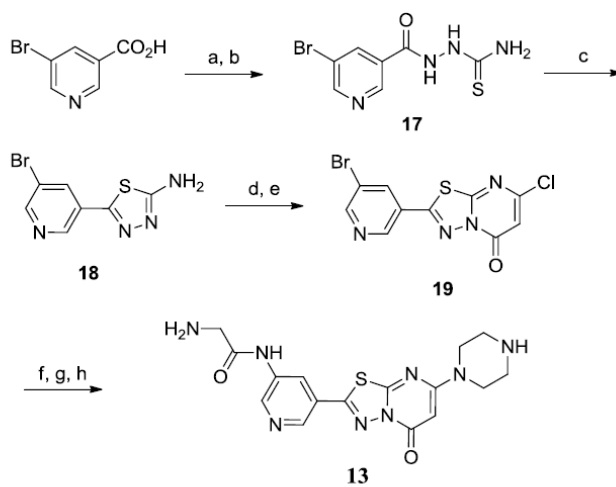


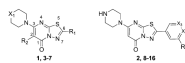
Figure 2. Visualization of MD simulations following 20 ns simulation trajectories of **2- α IIb β 3** (panel A), **14- α IIb β 3** (panel B), and **13- α IIb β 3** (panel C).



Reagents and conditions: (a) SOCl_2 , 1,2-DCE, DMF (cat), reflux, 12 h; (b) thiosemicarbazide, pyr, 0 °C to r.t.; (c) polyphosphoric acid (PPA) 100 °C then 17; (d) methyl-3-chloro-3-oxopropanoate, CH_3CN , 100 °C (μW); (e) POCl_3 , Hunig's base, 150 °C, (μW); (f) 1-Boc-piperazine, CH_3CN , Hunig's base, 100 °C (μW); (g) *tert*-butyl (2-amino-2-oxoethyl)carbamate, XantPhos (30 mol%), $\text{Pd}_2(\text{dba})_3$ (10 mol%), Cs_2CO_3 , 1,4-dioxane, 110 °C, (μW); (h) TFA/DCM.

Scheme 1.
Synthesis of 13.

Table 1

Platelet adhesion data as % inhibition at a set concentration and platelet aggregation data as IC₅₀'s.

Entry	R1	R2	XI	R3	X2	X3	Adhesion (% inhibition) ^a	Aggregation (IC ₅₀) ^b
tirofiban	NA	NA	NA	NA	NA	NA	88% (10 μM)	NP
eptifibatide	NA	NA	NA	NA	NA	NA	NP	0.012 μM
1	Ethyl	H	NH	NA	NA	NA	51% (20 μM)	4.0-10 μM
3	Ethyl	H	CH ₂	NA	NA	NA	23%(100 μM)	>100 μM
4	Ethyl	H	0	NA	NA	NA	20%(100 μM)	49 μM
5	Ethyl	H	NMe	NA	NA	NA	35%(100 μM)	>100 μM
6	Ethyl	F	NH	NA	NA	NA	41%(100 μM)	8.3 μM
7	tert-Butyl	H	NH	NA	NA	NA	35% (50 μM)	4.0 μM
8	NA	NA	NA	H	CH	CH	56%(100 μM)	3.0 μM
9	NA	NA	NA	COOH	CH	CH	37% (50 μM)	80 μM
10	NA	NA	NA	H	C-COOH	CH	49% (50 μM)	6.5 μM
11	NA	NA	NA	2-acetamidoacetic acid	CH	CH	78% (50 μM)	2.0 μM
12	NA	NA	NA	(S)-2-aminopropanamide	CH	CH	66% (100 μM)	5.87 μM
2 (RUC-2)	NA	NA	NA	2-aminoacetamide	CH	CH	83% (1 μM)	0.096 μM
13(RUC-4)	NA	NA	NA	2-aminoacetamide	CH	N	93% (1 μM)	0.045 μM
14 (RUC-3)	NA	NA	NA	2-aminoacetamide	N	CH	98% (1 μM)	0.033 μM
15	NA	NA	NA	2-aminoacetamide	CH	C-OH	69% (1 μM)	0.1 μM
16	NA	NA	NA	2-aminoacetamide	CH	C-CH ₂ OH	89% (1 μM)	0.075 μM

^a Adhesion assays were performed in triplicate at concentrations of 100 μM, 50 μM, 30 μM, 10 μM and/or 1 μM.

^b Aggregation assays performed in triplicate using adjusted dose ranges governed by potency. NA = not applicable. NP = not performed.

Table 2

Selected physicochemical and in vitro ADME profiles and pharmacokinetic analysis of 2 and 13.

Entry	Biological Stability ^a	Kinetic Solubility ^b	Thermodynamic Solubility ^b	hERG Inhibition ^c	CLint ($\mu\text{L}/\text{min}/\text{mg}$ protein) ^d	t _{1/2} (min.)
2 (RUC-2)	97.5 (15 min.)	35.8 (pH 6.6.)	41.8 (pH 6.6.)	< 5% @ 25 μM	0.684 (mouse)	> det. limit (mouse)
	93.3 (60 min.)	34.6 (pH 7.4)	28.0 (pH 7.4)		2.83 (rat)	> det. limit (rat)
	84.5 (120 min.)	36.1 (pH 8.5)	46.2 (pH 8.5)		-1.16 (human)	> det. limit (human)
		43.4 (pH 12)	>400 (pH 12)			
13(RUC-4)	100 (15 min.)	>57.8 (pH 6.6.)	340.4 (pH 6.6.)	< 5% @ 25 μM	89.0 (mouse)	15.6 (mouse)
	99.5 (60 min.)	>57.8 (pH 7.4)	239.5 (pH 7.4)		54.9 (rat)	25.3 (rat)
	91.7 (120 min.)	>57.8 (pH 8.5)	>400 (pH 8.5)		23.2 (human)	58.9 (human)
		>57.8 (pH 12)	>400 (pH 12)			

2 (RUC-2) Exposure Profile (IP)		Exposure Profile (IV)		13 (RUC-4) Exposure Profile (IP)		Exposure Profile (IV)	
Av. Weight (g)	27	Av. Weight (g)	27	Av. Weight (g)	27	Av. Weight (g)	27
Dose (mg)	0.03	Dose (mg)	0.03	Dose (mg)	0.03	Dose (mg)	0.03
Cmax ($\mu\text{M}/\text{mL}$)	0.222	CO ($\mu\text{g}/\text{mL}$)	1.354	Cmax ($\mu\text{g}/\text{mL}$)	0.405	CO ($\mu\text{g}/\text{mL}$)	1.145
Tmax (hr)	0.08	Tmax (hr)	NA	Tmax (hr)	0.08	Tmax (hr)	NA
AUC ($\mu\text{g}\cdot\text{hr}/\text{mL}$)	0.045	AUC (ng-hr/mL)	0.123	AUC ($\mu\text{g}\cdot\text{hr}/\text{mL}$)	0.087	AUC ($\mu\text{g}\cdot\text{hr}/\text{mL}$)	0.137
t _{1/2} (hr)	NA	t _{1/2} (hr)	0.07	t _{1/2} (hr)	NA	t _{1/2} (hr)	0.07
% Bioavailability ^e	36.8%			% Bioavailability ^e	63.5%		

^aBiological Stability assays were conducted in mouse plasma in triplicate.

^bKinetic solubility assays were performed in triplicate using both CLND and IHPLC methods (CLND methods are shown). Data was recorded in both ($\mu\text{g}/\text{mL}$ and μM ($\mu\text{g}/\text{mL}$ is shown).

^chERG channel inhibition was measured at 0.008 μM , 0.04 μM , 0.2 μM , 1.0 μM , 5.0 μM and 25.0 μM . Values were < 5% at all tested concentrations.

^dMicrosomal stability data (hepatocyte data not shown).

^eData represents measurements from 0 to 0.5 hours.